DOI: 10.1021/ic901481q

Inorganic Chemistry
Article

Vertex-Fused Metallaborane Clusters: Synthesis, Characterization and Electronic Structure of $[(\eta^5\text{-}C_5Me_5Mo)_3MoB_9H_{18}]$

Rajendra S. Dhayal,[†] Satyanarayan Sahoo,[†] K. Hari Krishna Reddy,[§] Shaikh M. Mobin,[‡] Eluvathingal D. Jemmis,[§,∥] and Sundargopal Ghosh*[,†]

[†]*Department of Chemistry, Indian Institute of Technology Madras, Chennai 600 036, India,* [‡]*National Single Crystal X-ray Diffraction Facility, Indian Institute of Technology Bombay, Mumbai 400 076, India,* [§]*Department of Inorganic and Physical Chemistry, Indian Institute of Science, Bangalore 560 022, India, and* [∥]*Indian Institute of Science Education and Research Thiruvananthapuram, CET Campus, Thiruvananthapuram, Kerala 695 016, India*

Received July 25, 2009

The reaction of the $[(\eta^5\text{-}C_5Me_5)MoCl_4]$ complex with $[LiBH_4\cdot THF]$ in toluene at −70 °C, followed by pyrolysis at 110 °C, afforded dark brown $[(\eta^5\text{-}C_5Me_5Mo)_3MoB_9H_{18}]$, **2**, in parallel with the known $[(\eta^5\text{-}C_5Me_5Mo)_2B_5H_9]$, **1**. Compound **2** has been characterized in solution by ^1H, ^{11}B, and ^{13}C NMR spectroscopy and elemental analysis, and the structural types were unequivocally established by crystallographic studies. The title compound represents a novel class of vertex-fused clusters in which a Mo atom has been fused in a perpendicular fashion between two molybdaborane clusters. Electronic structure calculations employing density functional theory yield geometries in agreement with the structure determinations, and on grounds of density functional theory calculations, we have analyzed the bonding patterns in the structure.

Introduction

The interest in polyhedral molecules ranges from transition-metal cluster compounds, with potential as a new generation of homogeneous and heterogeneous catalysts, to polyhedral boranes,[1] carboranes,[2] or metallaborane clusters. The extension of polyhedral boron-containing cluster chemistry beyond the constraints of single clusters of up to 15 vertices[3] is engendered by cluster fusion to generate macropolyhedral species.[4] Three complementary approaches to the expansion of cluster networks containing transition metal fragments have received much attention in metallaborane or metallacarborane chemistry:[5] for example, (i) condensation involving monoborane reagents,[6] (ii) insertion or fragmentation involving borane or metal carbonyl fragments,[7] and (iii) intercluster fusion of smaller tetrahedral, octahedral, and trigonal-prismatic fragments with two or more atoms held in common between the constituent subclusters.[8] One advantage offered by the study of metallaborane clusters is that the limited bonding capabilities of the borane fragment can be used to circumscribe the behavior of the metal fragment.

After it had been discovered that the reaction of the hydrogen-rich $[(\eta^5\text{-}C_5Me_5WH_3)B_4H_8]$ with $[BH_3\cdot THF]$ led to the isolation of $[(\eta^5\text{-}C_5Me_5W)_2B_5H_9]$, $[(\eta^5\text{-}C_5Me_5W)_2B_6H_{10}]$, $[(\eta^5\text{-}C_5Me_5W)_2B_7H_9]$, and $[(\eta^5\text{-}C_5Me_5W)_3(\mu\text{-}H)B_8H_8]$

*To whom correspondence should be addressed. Fax: (+91) 44 2257 4202. E-mail: sghosh@iitm.ac.in.

(1) (a) Muetterties, E. L., Ed. *Boron Hydride Chemistry*; Academic Press: New York, 1975. (b) Brown, L. D.; Lipscomb, W. N. *Inorg. Chem.* **1977**, *16*, 2989. (c) Schleyer, P. v. R.; Najafian, K.; Mebel, A. M. *Inorg. Chem.* **1998**, *37*, 6765.

(2) (a) Zi, G.; Li, H.-W.; Xie, Z. *Organometallics* **2001**, *20*, 3836. (b) Zi, G.; Li, H.-W.; Xie, Z. *Chem. Commun.* **2001**, 1110. (c) Zi, G.; Li, H.-W.; Xie, Z. *Organometallics* **2002**, *21*, 5415. (d) Grimes, R. N. *Angew. Chem., Int. Ed.* **2003**, *42*, 1198. (e) Xie, Z. *Pure Appl. Chem.* **2003**, *75*, 1335. (f) Hosmane, N. S.; Maguire, J. A. *Organometallics* **2005**, *24*, 1356. (g) Deng, L.; Chan, H.-S.; Xie, Z. *Angew. Chem., Int. Ed.* **2005**, *44*, 2128. (h) Deng, L.; Chan, H.-S.; Xie, Z. *J. Am. Chem. Soc.* **2006**, *128*, 5219. (i) Zhang, J.; Deng, L.; Chan, H.-S.; Xie, Z. *J. Am. Chem. Soc.* **2007**, *129*, 18. (j) King, R. B. *J. Organomet. Chem.* **2007**, *692*, 1773.

(3) (a) Burke, A.; Ellis, D.; Giles, B. T.; Hodson, B. E.; Macgregor, S. A.; Rosair, G. M.; Welch, A. J. *Angew. Chem., Int. Ed.* **2003**, *42*, 225. (b) Deng, L.; Xie, Z. *Organometallics* **2007**, *26*, 1832 and references therein.

(4) (a) Burdett, J. K.; Canadell, E. *J. Am. Chem. Soc.* **1990**, *112*, 7207. (b) Shea, S. L.; Bould, J.; Londesborough, M. G. S.; Perera, S. D.; Franken, A.; Ormsby, D. L.; Jelinek, T.; Stibr, B.; Holub, J.; Kilner, C. A.; Thornton-Pett, M.; Kennedy, J. D. *Pure Appl. Chem.* **2003**, *75*, 1239. (c) Carr, M. J.; Perera, S. D.; Jelinek, T.; Stibr, B.; Clegg, W.; Kilner, C. A.; Kennedy, J. D. *Chem. Commun.* **2007**, 3559.

(5) (a) Corbett, J. D. *Acc. Chem. Res.* **1981**, *14*, 239. (b) Mingos, D. M. P. *J. Chem. Soc., Chem. Commun.* **1983**, 706. (c) Kennedy, J. D. *Prog. Inorg. Chem.* **1984**, *32*, 519. (d) Kennedy, J. D. *Prog. Inorg. Chem.* **1986**, *34*, 211.

(6) (a) Fehlner, T. P. *J. Chem. Soc., Dalton Trans.* **1998**, 1525. (b) Fehlner, T. P. *Organometallics* **2000**, *19*, 2643. (c) *Molecular Clusters A Bridge to Solid-State Chemistry*; Fehlner, T. P., Halet, J.-F., Saillard, J.-Y., Eds.; Cambridge University Press: Cambridge, U. K., 2007.

(7) Ghosh, S.; Fehlner, T. P.; Noll, B. C. *Chem. Commun.* **2005**, 3080.

(8) (a) Wong, K.-S.; Bowser, J. R.; Pipal, J. R.; Grimes, R. N. *J. Am. Chem. Soc.* **1978**, *100*, 5045. (b) Mingos, D. M. P. *Acc. Chem. Res.* **1984**, *17*, 311. (c) Grimes, R. N. *Coord. Chem. Rev.* **1995**, *143*, 71. (d) Kennedy, J. D. In *Advances in Boron Chemistry*; Siebert, W., Ed.; Royal Society of Chemistry: Cambridge, U. K., 1997; p 451.

Published on Web 01/05/2010

Scheme 1

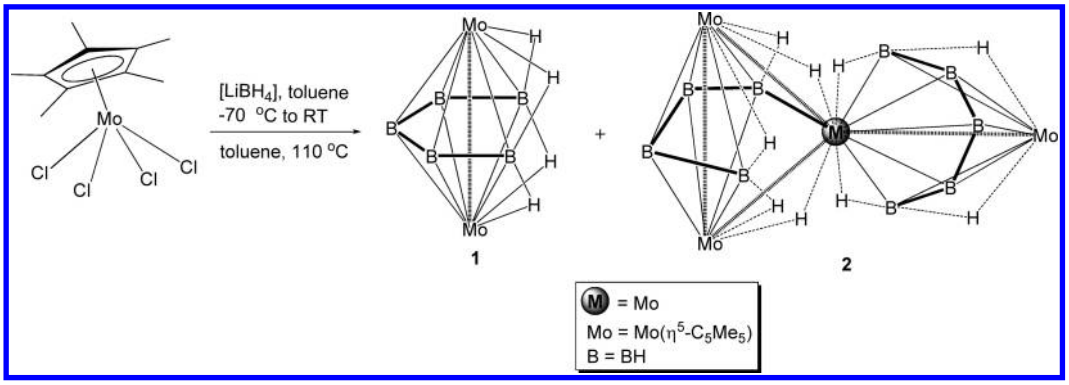

clusters,[9,10] a reinvestigation of a related molybdenum system became of interest. As the results obtained with the tungsten complex suggested that higher nuclearity clusters than previously thought might now be accessible, we pursued this chemistry in the molybdenum system. The objective of generating higher nuclearity molybdaborane clusters was not achieved, the only major product being **1**.[11,12] However, an interesting fused cluster was isolated, as a minor byproduct. In this report, we now account for the structure and bonding of a novel vertex-fused molybdaborane cluster, **2**. Also, to provide some new insight into the nature of bonding in the fused cluster, particularly the long and short Mo−Mo internuclear distances, density functional theory (DFT) calculations were carried out.

Results and Discussion

Treatment of the $[(\eta^5\text{-}C_5Me_5)MoCl_4]$ complex with $[LiBH_4\cdot THF]$ in toluene at −70 °C, followed by pyrolysis at 110 °C, affords dark brown **2** in parallel with known **1** (Scheme 1). Compound **2** has been isolated in modest yield and characterized spectroscopically as well as by single-crystal X-ray diffraction analysis.

A solid-state structure determination of **2**, shown in Figure 1, shows two bicapped trigonal bipyramidal (btbp) cages fused in a perpendicular fashion with one molybdenum atom common to both core skeletons. The outer Mo atoms, which occupy the equatorial positions of the individual trigonal plane, are η^5-coordinated to the C_5Me_5 ligand. The inner Mo atom which is fused between two clusters has two bridging hydrogen atoms, one bound to Mo1 and the other one with the Mo2 center (Figure 1). Consequently, each of the fused clusters resembles the structure of **1**, and there is a close correspondence between most of the structural parameters of **2** and those of **1**. The average B−B distance of 1.70 Å in **2** is shorter in comparison to that of **1** (1.72 Å). Two of the Mo−Mo bond distances in **2** (viz., Mo(2)−Mo(3) = 3.0481(5) and Mo(1)−Mo(3) = 3.0247(5) Å, Figure 1) are significantly longer than in **1** {2.8085(6) Å},[12] reflecting a notably different environment of the unique Mo atom. A similar kind of behavior was also observed in [{1-(Cp*Ru)(μ-H)B_4H_9}$_2$Ru] in which each of the fused clusters resembles the parent cluster from which it was derived.

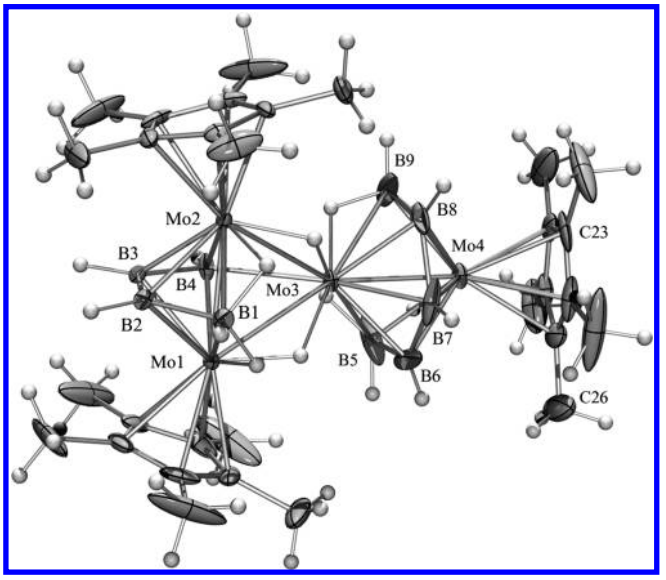

Figure 1. Molecular structure of $[(\eta^5\text{-}C_5Me_5Mo)_3MoB_9H_{18}]$ (**2**). The thermal ellipsoids correspond to 30% probability. Selected interatomic distances (Å): Mo(1)−Mo(2), 2.8256(5); Mo(1)−Mo(3), 3.0247(5); Mo(2)−Mo(3), 3.0481(5); Mo(3)−Mo(4), 2.8391(5); B(1)−B(2), 1.731(7); B(2)−B(3), 1.676(7); B(5)−B(6), 1.724(17); B(6)−B(7), 1.665(14); Mo(1)−B(1), 2.317(5); Mo(1)−B(3), 2.221(5); Mo(2)−B(2), 2.212(5); Mo(2)−B(4), 2.301(5); Mo(3)−B(4), 2.477(5); Mo(3)−B(5), 2.327(7); Mo(3)−B(9), 2.332(8); Mo(4)−B(6), 2.158(7); Mo(4)−B(8), 2.181(7).

The major difference between [{1-(Cp*Ru)(μ-H)B_4H_9}$_2$-Ru] and **2** is that the former has a shorter metal−metal bond distance {2.7930(10) Å} compared to the parent metallaborane [1,2-(Cp*Ru)$_2$(μ-H)B_4H_9] {2.8527(4) Å}, while the latter has longer metal−metal bond distances {3.0481(5)Å, 3.0247(5)Å} compared to its parent metallaborane **1** {2.8085(6) Å}. The intracluster Mo−Mo bond distances of 2.8256(5) and 2.8391(5) Å in **2** are distinctly longer than those reported in $[(\eta^5\text{-}C_5Me_5MoCl)_2B_2H_6]$[11] and $[(\eta^5\text{-}C_5Me_5Mo)_2B_5H_7(\mu_3\text{-}OEt)]$;[13] however, they are comparable to those observed in $[(\eta^5\text{-}C_5Me_5Mo)_2B_5H_9]$[12,14] or $[(\eta^5\text{-}C_5Me_5Mo)_2B_5H_5Cl_4]$.[15]

The spectroscopic data of **2** are fully in accord with the solid-state structure, and no evidence of fluxional behavior is

(9) (a) Weller, A. S.; Shang, M.; Fehlner, T. P. *Organometallics* **1999**, *18*, 53. (b) Weller, A. S.; Shang, M.; Fehlner, T. P. *Organometallics* **1999**, *18*, 853.
(10) Bose, S. K.; Ghosh, S.; Noll, B. C.; Halet, J.-F.; Saillard, J.-Y.; Vega, A. *Organometallics* **2007**, *26*, 5377.
(11) Aldridge, S.; Shang, M.; Fehlner, T. P. *J. Am. Chem. Soc.* **1998**, *120*, 2586.
(12) Kim, D. Y.; Girolami, G. S. *J. Am. Chem. Soc.* **2006**, *128*, 10969.
(13) Sahoo, S.; Dhayal, R. S.; Varghese, B.; Ghosh, S. *Organometallics* **2009**, *28*, 1586.
(14) Aldridge, S.; Hashimoto, H.; Kawamura, K.; Shang, M.; Fehlner, T. P. *Inorg. Chem.* **1998**, *37*, 928.
(15) Dhayal, R. S.; Sahoo, S.; Ramkumar, V.; Ghosh, S. *J. Organomet. Chem.* **2009**, *694*, 237.

Chart 1

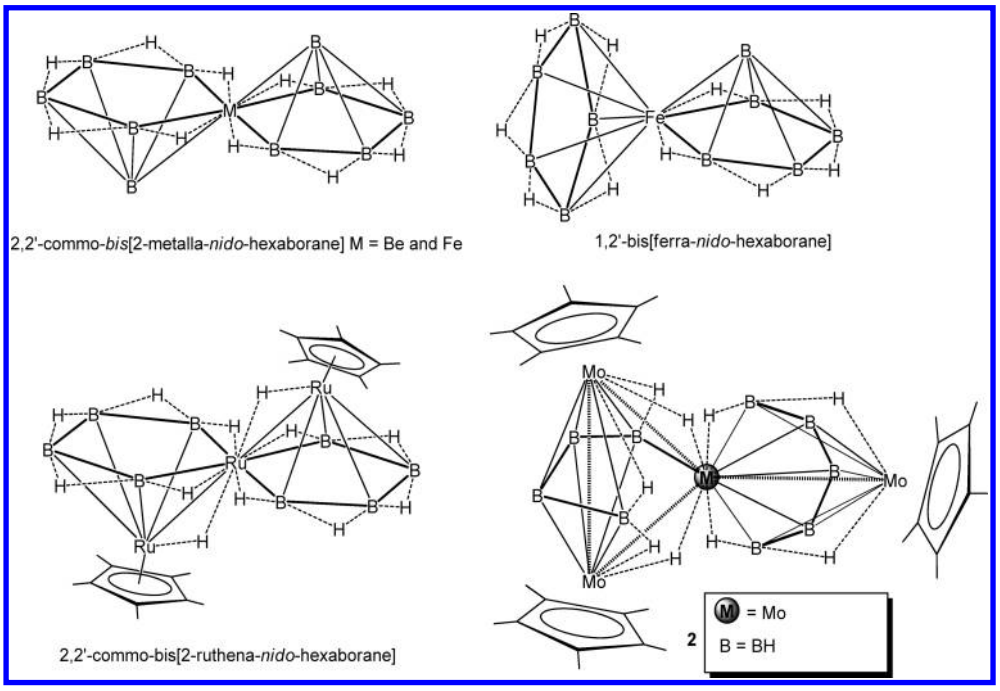

observed. The IR spectrum of **2** features strong bands at 2480 and 2458 cm^{-1} due to terminal B−H stretches. The molecular ion peak in the fast-atom bombardment (FAB) mass spectrum corresponds to $[(\eta^5\text{-}C_5Me_5Mo)_3MoB_9H_{18}]$. The NMR data for **2** indicate an unsymmetrical structure with inequivalent cluster units in solution. Thus, the ^{1}H NMR spectrum of **2** shows two different singlets for the Cp* fragments (Cp* = η^5-C_5Me_5) appeared, each at δ = 2.06 and 2.09 ppm in a ratio of 1:2. The ^{11}B NMR chemical shifts as well as the ^{1}H shifts of the terminal hydrogen atoms correspond closely to those of the comparable atoms of **1**. The Mo−H−Mo protons and the distinct Mo(2)−H−B(4) proton, as shown in Scheme 1, appeared at δ = −12.62 and −6.26 ppm, respectively. The ^{1}H resonance at −7.43 ppm has been assigned to the four Mo−H−B protons [Mo(1)−H−B(1), Mo(2)−H−B(1), Mo(4)−H−B(5), and Mo(4)−H−B(9), Figure 1]. The ^{1}H resonances of the protons that bridge B5 and B9 and the central Mo3 atom appear at δ = −9.62 ppm, thereby inverting their relative positions in the spectrum compared to that of **1**. These differences also reflect the distinctly different electronic environment of the unique metal center of **2** relative to **1**.

The geometry of **2** is unique from the standpoint of the structure of the resulting boron cage and the environment of the fused central molybdenum atom. In view of the interest in the structure of **2**, it is interesting to note that **2** exhibits characteristics similar to, but different from, those of [1,2′- and 2,2′-$B_5H_{10}FeB_5H_{10}$],[16] [2,2′-$B_5H_{10}BeB_5H_{10}$],[17] and [{1-(Cp*Ru)(μ-H)B_4H_9}$_2$Ru],[18] reported earlier by the groups of Grimes, Gaines, and Fehlner, respectively. As shown in Chart 1, the solid-state structures of these complexes show that two pentagonal pyramid cages fused in a transoid or perpendicular fashion with one atom common to both core skeletons. The dihedral angle of 91° between the basal planes of the two boron cages of **2**, placing one of the equatorial molybdenum fragments into the main boron framework, clearly shows that two of the btbp units fused in a perpendicular fashion.

It has become apparent in recent years that a large number of transition metal−carbonyl clusters, boranes as well as carboranes, have been synthesized by the condensation or fusion of smaller cluster fragments.[5,7] These cluster types lead to extensions of the electron counting rules.[19] In the Mingos approach, these condensation processes occur by vertex-, edge-, or face-sharing.[8b] The total electron count in such a condensed cluster is equal to the sum of the electron counts for the parent polyhedra minus the electron count of the shared unit (atom, pair of atoms, etc.). The condensed polyhedron is viewed as a complex between two individual polyhedra with one polyhedron acting as a ligand toward the second polyhedron. Thus, in terms of counting cluster valence electrons (cve), the formal disproportionation, as shown in eq 1, based on the condensation principle is self-evident. Therefore, as shown in eq 1, **2** can be viewed as formed from the condensation of six sep $[(\eta^5\text{-}C_5Me_5Mo)_2B_4H_{10}]$ and $[(\eta^5\text{-}C_5Me_5Mo)_2B_5H_9]$ with the elimination of Cp*H.

$$\begin{array}{rcl} & (Cp*Mo)_2B_4H_{10} + (Cp*Mo)_2B_5H_9 \rightarrow & \\ \text{cve} = & 44 \qquad\qquad 46 & \\ & (Cp*Mo)_3MoB_9H_{18} + Cp*H & \\ & 84 \qquad\quad 6 & \end{array} \qquad (1)$$

(16) (a) Weiss, R.; Grimes, R. N. *J. Am. Chem. Soc.* **1977**, *99*, 8087. (b) Weiss, R.; Grimes, R. N. *Inorg. Chem.* **1979**, *18*, 3291. (c) Gilbert, K. B.; Boocock, S. K; Shore, S. G. In *Comprehensive Organometallic Chemistry*; Wilkinson, G., Stone, F. G. A., Abel, E., Eds.; Pergamon Press: Oxford, U. K., 1982; Vol. *5*, p 879. (d) Mebel, A. M.; Musaev, D. G.; Koga, N.; Morokuma, K. *Bull. Chem. Soc. Jpn.* **1993**, *66*, 3259.

(17) (a) Gaines, D. F.; Walsh, J. L. *Inorg. Chem.* **1978**, *17*, 1238. (b) Gaines, D. F.; Walsh, J. L.; Calabrese, J. C. *Inorg. Chem.* **1978**, *17*, 1242.

(18) Lei, X.; Shang, M.; Fehlner, T. P. *Angew. Chem., Int. Ed.* **1999**, *38*, 1986.

(19) (a) Wade, K. *Inorg. Nucl. Chem. Lett.* **1972**, *8*, 559. (b) Wade, K. *Adv. Inorg. Chem. Radiochem.* **1976**, *18*, 1. (c) Wade, K. *Adv. Inorg. Chem. Radiochem.* **1976**, *18*, 67. (d) Mingos, D. M. P. *Nature* (*London*) **1972**, *236*, 99.

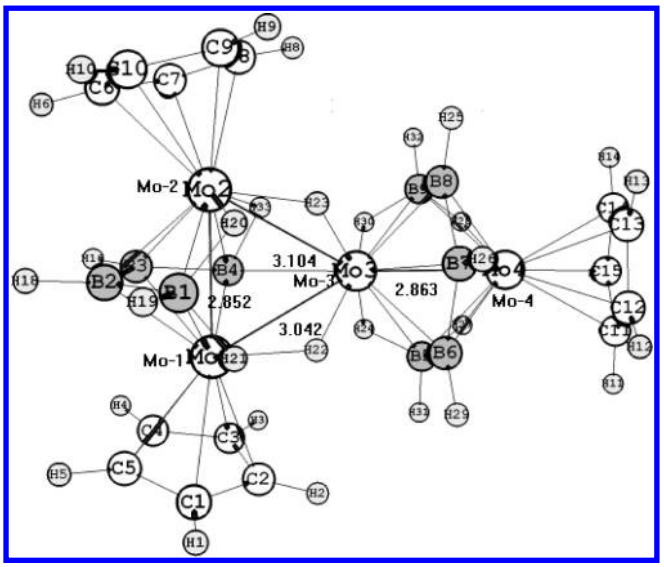

Figure 2. Optimized structure of $[(\eta^5\text{-}C_5Me_5Mo)_3MoB_9H_{18}]$, **2**, using the B3LYP method and LANL2DZ basis set. Different Mo−Mo internuclear distances which range between bonding and nonbonding interactions are highlighted.

We have also applied the *mno* electron counting rule[20] to **2**. The number of skeletal electron pairs required for this structure is *m* (number of individual polyhedral fragments) + *n* (number of vertexes in the polyhedron) + *o* (number of single vertex sharing junctions) + *p* (number of missing vertexes in the idealized closo skeleton). Here, $m = 5$, $n = 28$, $o = 4$, and $p = 5$. Thus, according to this rule, **2** needs 42 skeletal electron pairs for the cluster bonding. The total number of electron pairs available in **2** is 48 [3 × Cp* (45e) + 9 × BH (18e) + 9 × μH (9e) + 4 × Mo (24e) = 92e, i.e., 48 electron pairs]. We subtract two electron pairs corresponding to two Mo−Mo bonds, leading to 46 electron pairs. The extra four-electron pairs are perhaps more localized on the metal centers and not involved in skeletal bonding. Indeed, in our natural bond orbital (NBO) analysis, we found a lone pair on each molybdenum with significant d character.

Notably, the pathway for the formation of **2** has not been established; however, note that, during the metathesis reaction of $[(\eta^5\text{-}C_5Me_5)MoCl_4]$ with borohydrides, $[(\eta^5\text{-}C_5Me_5Mo)_2B_4H_{10}]$ could be one of the intermediate species leading to **1**.[11] Therefore, compound **2** has been postulated to be generated from the condensation of $[(\eta^5\text{-}C_5Me_5Mo)_2B_4H_{10}]$ and **1** at an elevated temperature.

Computational Studies. One of the most interesting aspects of the structure of **2** is the differences in Mo−Mo internuclear distances that range between bonding and nonbonding interactions. In an effort to understand the nature of various Mo−Mo interactions, theoretical studies using extended Huckel theory and DFT methods were carried out on structure **2**. The model of the electronic structure that develops demonstrates the factors behind the variations in Mo−Mo distances (Figure 2).

The variation in the first set of bond distances containing intracluster bonds, Mo(1)−Mo(2) (2.852 Å) and Mo(3)−Mo(4) (2.863 Å), can be rationalized as follows. Fehlner and co-workers[14] argued that a central

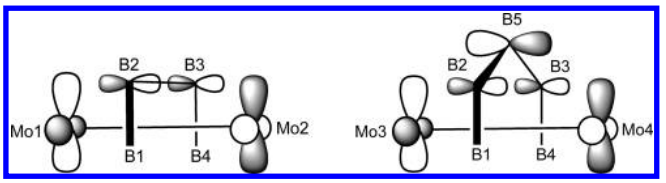

Figure 3. Metal orbital interactions with boron in a four- and five-membered middle ring. In the five-membered middle ring case (right), the δ^* MO of the metal interacts with the p orbital of the boron (B5) in a bonding fashion.

five-membered ring is more favorable as compared to a four-membered ring for a metal−metal interaction. We have found a similar bonding pattern in our case, and as shown in Figure 3, the extra boron atom in the five-membered ring (B5) interacts in a bonding fashion with the δ antibonding orbital of the metals. Subsequently, the Mo(3)−Mo(4) bond having a B5 middle ring should be shorter compared to that of the Mo(1)−Mo(2) bond having a B4 middle ring.

We have observed that the trend in bond lengths is reversed in this case. It is due to the fact that Mo(1) and Mo(2) have a bonding interaction with Mo(3), which is a considerably stronger interaction than the bonding interaction provided by the extra boron in the five-membered ring. The intercluster Mo−Mo bonds (Mo(1)−Mo(3) (3.042 Å) and Mo(2)−Mo(3) (3.104 Å), involve various multicenter bonding patterns. Further, in the core of **2**, there exist three different 3c−2e bonds, Mo(1)−Mo(3)−B(4), Mo(1)−H(22)−Mo(3), and Mo(2)−H(23)−Mo(3).

Conclusion

In summary, a novel vertex-fused molybdaborane cluster, **2**, has been discovered, which is remarkable enough in being a hydrogen-rich cluster, but its thermodynamic stability, together with its stability in air, makes it unique. The available synthetic routes to the preparation of fused clusters are often time-consuming, technically challenging, and low in yield. However, compound **2** has been isolated in modest yield (21%). The variation in Mo−Mo bond distances in **2** that range between bonding and nonbonding interactions is analyzed in detail.

Experimental Section

General Procedures and Instrumentation. All of the operations were conducted under an Ar/N_2 atmosphere using standard Schlenk techniques. Solvents were distilled prior to use under argon. MeI was freshly distilled prior to use; all other reagents (Aldrich) were used as received. $[(\eta^5\text{-}C_5Me_5)MoCl_4]$ was prepared with some modification[15] of Green and co-workers'[21] work. The external reference, $[Bu_4N(B_3H_8)]$,[22] for the ^{11}B NMR was synthesized according to the literature method. Chromatography was carried out on 3 cm of silica gel in a 2.5 cm dia column. Thin layer chromatography was carried on 250 mm dia aluminum supported silica gel TLC plates (MERCK TLC Plates). NMR spectra were recorded on 400 and 500 MHz Bruker FT-NMR spectrometers. Residual solvent protons were used as a reference (δ, ppm, $CDCl_3$, 7.26), while a sealed tube containing $[Bu_4N(B_3H_8)]$ in C_6D_6 (δB, ppm, −30.07) was used as an external reference for the ^{11}B NMR. Infrared spectra were obtained on a Nicolet 6700 FT-IR spectrometer.

(20) (a) Jemmis, E. D.; Balakrishnarajan, M. M.; Pancharatna, P. D. *J. Am. Chem. Soc.* **2001**, *123*, 4313. (b) Jemmis, E. D.; Balakrishnarajan, M. M.; Pancharatna, P. D. *Chem. Rev.* **2002**, *102*, 93.

(21) Green, M. L. H.; Hubert, J. D.; Mountford, P. *J. Chem. Soc., Dalton Trans.* **1990**, 3793.

(22) Ryschkewitsch, G. E.; Nainan, K. C. *Inorg. Synth.* **1975**, *15*, 113.

Mass spectra were obtained on a Jeol SX 102/Da-600 mass spectrometer/Data System using Argon/Xenon (6 kV, 10 mÅ) as the FAB gas.

Computational Methods. The structure was optimized using the Gaussian 03 suite of programs.[23] Full molecular geometry optimization was performed by means of Becke's three-parameter hybrid method using the LYP correlation functional (B3LYP),[24] which combines the Hartree−Fock exchange term with the DFT exchange-correlation terms. The basis set employed is LANL2DZ.[25] The WinCacao program[26] is used for extended Huckel molecular orbital studies. NBO[27] methods are used to analyze the bonding patterns.

Synthesis of 2. To $[(\eta^5\text{-}C_5Me_5)MoCl_4]$ (0.5 g, 1.34 mmol) in 20 mL of toluene was added a 6-fold excess of $LiBH_4\cdot THF$ (4.02 mL, 8.05 mmol) at −70 °C. The mixture was stirred at room temperature for 1 h. After the removal of toluene, the residue was extracted into hexane. The extract was filtered through a frit using Celite. The yellowish green hexane extract was dried and taken in 25 mL of toluene and thermolyzed at 110 °C for 20 h. The solvent was removed in vacuo; the residue was extracted into hexane and passed through Celite. After the removal of solvent from the filtrate, the residue was subjected to a chromatographic workup using silica gel TLC plates. Elution with hexane/CH_2Cl_2 (90:10 v/v) yielded in the following order orange **1**, (0.34 g, 48%), dark brown **2** (0.26 g, 21%), and a trace amount of two orange-red oxamolybdaboranes,[13] $[(\eta^5\text{-}C_5Me_5Mo)_2B_5(\mu_3\text{-}OEt)H_6R]$ (R = H and R = *n*-BuO).

Note that **1** has been characterized by comparison of its spectroscopic data reported by Aldridge et.al.[28]

Selected data for **2**. MS (FAB) P^+(max): *m*/*z* (%) 905 (isotopic pattern for 4Mo, 9B atoms). ^{11}B NMR (128.3 MHz, $CDCl_3$, 22 °C): δ 62.7 (br, 2B), 59.1 (br, 2B), 56.3 (d, J_{B-H} = 133 Hz, 1B), 51.1 (d, J_{B-H} = 131 Hz, 1B), 25.1 (br, 2B), 23.5 (d, J_{B-H} = 141 Hz, 1B). ^{1}H NMR (400 MHz, $CDCl_3$, 22 °C): δ 5.84 (partially collapsed quartet (pcq), $1BH_t$), 4.65 (pcq, $2BH_t$), 4.28 (pcq, $1BH_t$), 4.16 (pcq, $2BH_t$), 3.98 (pcq, $1BH_t$), 3.93 (pcq, $1BH_t$), 3.73 (pcq, $1BH_t$), 2.09 (s, 30H, 2Cp*), 2.06 (s, 15H, 1Cp*), −6.26 (br, 1Mo−*H*−B), −7.43 (br, 4Mo−*H*−B), −9.62 (br, 2Mo−*H*−B), −12.62 (br, 2Mo−*H*−Mo). ^{13}C NMR (125.7 MHz, $CDCl_3$, 22 °C): δ 108.84, 107.27 (s, η^5-*C*$_5$Me$_5$), 13.11, 12.74 (s, η^5-C$_5$*Me*$_5$). IR (hexane, cm^{-1}): 2480 m, 2458 m (BH_t). Anal. Calcd for $C_{31}H_{64}B_9Mo_4Cl$: C, 39.06; H, 6.77. Found: C, 38.67; H, 7.03.

X-Ray Structure Determination. Suitable X-ray-quality crystals of **2** were grown by the slow diffusion of a hexane/CH_2Cl2 (9.5:0.5 v/v) solution, and single-crystal X-ray diffraction studies were undertaken. Crystal data were collected and integrated using an Oxford Diffraction Xcalibur-S CCD system equipped with graphite monochromated Mo Kα (λ = 0.71073 Å) radiation at 150 K. The structure was solved by heavy atom methods using SHELXS-97[29] and refined using SHELXL-97[30] (Sheldrick, G. M., University of Göttingen). The molecular structure was drawn using ORTEP-3. The non-hydrogen atoms were refined with anisotropic displacement parameters. All hydrogens could be located in the difference Fourier map. However, the hydrogen atoms bonded to carbons and borons were fixed at chemically meaningful positions and were allowed to ride with the parent atom during the refinement.

Crystal data for **2** (0.5 CH_2Cl_2). Crystal system, space group: tetragonal, *P*4(2)/*n*. Unit cell dimensions, a = 24.1435(2) Å, b = 24.1435(2) Å, c = 13.8299(2) Å, Z = 8. Density (calculated): 1.559 Mg/m^3. Final R indices [$I > 2\sigma(I)$]: R1 = 0.0316, wR2 = 0.0712. Reflections collected, 59 723; independent reflections, 7090 [R(int) = 0.0547]; goodness of fit on F^2, 0.904.

Acknowledgment. Generous support of the Department of Science and Technology, DST (Grant No. SR/S1/IC-19/2006) is gratefully acknowledged. We thank Dr. Babu Varghese for helpful discussions on X-ray Crystallography. We would also like to thank Mass Lab, SAIF, CDRI, Lucknow 226001, India for FAB mass analysis and Single Crystal XRD Facility, Indian Institute of Technology Bombay, Mumbai 400 076, India. R.S.D. and S.S. thank the University Grants Commission, India, for a junior and senior research fellowship, respectively.

Supporting Information Available: CIF file for **2** and *xyz* coordinates of the completely optimized structure **2** using the B3LYP functional and LANL2DZ basis set. This material is available free of charge via the Internet at http://pubs.acs.org

(23) Frisch, J.; Trucks, G. W.; Schlegel, H. B.; Scuseria, G. E.; Robb, M. A.; Cheeseman, J. R.; Montgomery, J. A., Jr.; Vreven, T.; Kudin, K. N.; Burant, J. C.; Millam, J. M.; Iyengar, S. S.; Tomasi, J.; Barone, V.; Mennucci, B.; Cossi, M.; Scalmani, G.; Rega, N.; Petersson, G. A.; Nakatsuji, H.; Hada, M.; Ehara, M.; Toyota, K.; Fukuda, R.; Hasegawa, J.; Ishida, M.; Nakajima, T.; Honda, Y.; Kitao, O.; Nakai, H.; Klene, M.; Li, X.; Knox, J. E.; Hratchian, H. P.; Cross, J. B.; Adamo, C.; Jaramillo, J.; Gomperts, R.; Stratmann, R. E.; Yazyev, O.; Austin, A. J.; Cammi, R.; Pomelli, C.; Ochterski, J. W.; Ayala, P. Y.; Morokuma, K.; Voth, G. A.; Salvador, P.; Dannenberg, J. J.; Zakrzewski, V. G.; Dapprich, S.; Daniels, A. D.; Strain, M. C.; Farkas, O.; Malick, D. K.; Rabuck, A. D.; Raghavachari, K.; Foresman, J. B.; Ortiz, J. V.; Cui, Q.; Baboul, A. G.; Clifford, S.; Cioslowski, J.; Stefanov, B. B.; Liu, G.; Liashenko, A.; Piskorz, P.; Komaromi, I.; Martin, R. L.; Fox, D. J.; Keith, T.; Al-Laham, M. A.; Peng, C. Y.; Nanayakkara, A.; Challacombe, M.; Gill, P. M. W.; Johnson, B.; Chen, W.; Wong, M. W.; Gonzalez, C.; Pople, J. A. *Gaussian 03*; Gaussian, Inc.: Pittsburgh, PA, 2003.

(24) (a) Becke, A. D. *J. Chem. Phys.* **1993**, *98*, 5648. (b) Becke, A. D. *Phys. Rev. A* **1988**, *38*, 3098. (c) Lee, C.; Yang, W.; Parr, R. G. *Phys. Rev. B* **1988**, *37*, 785.

(25) (a) Hay, P. J.; Wadt, W. R. *J. Chem. Phys.* **1985**, *82*, 270. (b) Wadt, W. R.; Hay, P. J. *J. Chem. Phys.* **1985**, *82*, 284. (c) Hay, P. J.; Wadt, W. R. *J. Chem. Phys.* **1985**, *82*, 299.

(26) Maelli, C.; Proserpio, D. M. *J. Chem. Educ.* **1990**, *67*, 399.

(27) Reed, A. E.; Curtiss, L. A.; Weinhold, F. *Chem. Rev.* **1988**, *88*, 899.

(28) Aldridge, S.; Fehlner, T. P.; Shang, M. *J. Am. Chem. Soc.* **1997**, *119*, 2339.

(29) Sheldrick, G. M. *SHELXS-97*; University of Göttingen: Göttingen, Germany, 1997.

(30) Sheldrick, G. M. *SHELXL-97*; University of Göttingen: Göttingen, Germany, 1997.